KSME International Journal, Vol. 12, No. 5, pp. 827~835, 1998

Small Punch Tests on Steels for Steam Power Plant (II)
— Modeling —

Eric Fleury* and Jeong Soo Ha*
(Received October 17, 1997)

Analytical formulations using uniaxial tensile stress-strain constitutive behavior have been proposed to model the elastic bending, plastic bending and membrane stretching regimes of small punch load-deflection curves. The equations have been applied on austenitic 12Cr-1Mo steel in the temperature range 25°-600°C and have been verified on ferritic 1Cr-0.5Mo steel at T=25°C. Using these formulations, the room temperature uniaxial tensile stress-strain behavior of the ferritic 2.25Cr-1Mo steel has been determined from the small punch load-deflection response.

Key Words: Small Punch Test, Modeling, Elastic Bending, Plastic Bending, Membrane Stretching.

1. Introduction

In the late 70s-early 80s, studies have focused on the characterization of the mechanical properties of metals from miniature samples. Because engineers are often limited by the size of testing components, development of special mechanical testing techniques from miniature-size specimens were required to assess material characteristics. Since its development, small punch test (SP) has been investigated mainly to identify ductility loss in steels due to temper or irradiation embrittlement (Huang *et al.*, 1982, Baik *et al.*, 1986, Mao *et al.*, 1987, Foulds et al., 1994).

Using elastic-plastic finite element, Manahan et al. (1981) were the first authors to proposed a modeling of the load versus deflection curve in small punch experiments. Huang et al. (1982) obtained a good agreement between bending ductilities and tensile ductilities for several irradiated alloys. Following these results, further studies were investigated showing good agreement of the mechanical properties (yield stress, strain hardening, and ultimate tensile strength) as determined by small punch test and uniaxial tensile test (Lucas et al., 1990, Ha et al., 1998).

Consequently, the small punch test is potentially capable to provide informations of the stress-strain behavior using a specimen removed from real components. This offers great resources as to assess the mechanical properties of unknown materials, or materials with unknown heat-treatment, and to evaluate the degradation of the mechanical properties of in-service materials.

As previously described by Baik et al. (1986), the small punch load-deflection response can be partitioned into four regimes corresponding to elastic bending deformation associated with local surface micro-yielding, plastic bending deformation, membrane stretching, and plastic instability.

Simulation of the load-deflection curve, using analytical expressions, was proposed by Onat *et al.* (1956) and applied by Mao *et al.* (1987). This approach assumed a perfect rigid plastic behavior to describe the small punch load-deflection response at room temperature. If in the plastic bending regime, a good agreement was obtained with experiment, the formulation failed to give an accurate description of the small punch test behavior in the membrane stretching regime.

In this present work, an analysis developed by Wang (1970) of the membrane stretching has

* Power Generation Research Laboratory K. E. P. R. I., Taejon

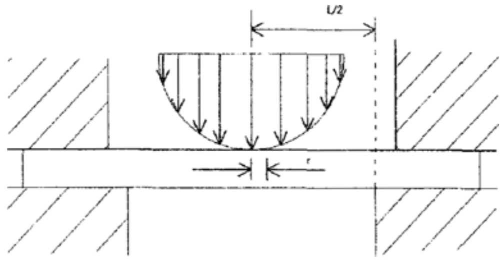

Fig. 1 Schematic representation of the applied load on a SP specimen.

been employed to examine the behavior of small punch test in the temperature range 25° to 600°C. The formulation has also been used to evaluate the uniaxial stress-strain behavior on a ferritic steel.

2. Analysis of the Small Punch Test Load-Deflection Response.

2.1 Elastic regime

In the first portion of the load-deflection response, two distinct modes of deformation take place simultaneously: a) penetration of the ball within the specimen surface (indeed local micro-yielding), b) elastic bending deformation.

a) The penetration of the indenter into a flat plate can be calculated from the dimension of the contact area. In the case of a sphere, the major and minor axis of the contact can be determined from the equation as given in handbook (Pilkey, 1994) :

$$a = b = 0.721\,(Fd_1\gamma)^{1/3} \qquad (1)$$

where a and b are the radius of the contact area, F = the applied load, d_1 = the diameter of the indenter, and with:

$$\gamma = \frac{(1-\nu_1^2)}{E_1} \quad \frac{(1-\nu_2^2}{E_2} \qquad (2)$$

where E_1, E_2, ν_1 and ν_2 are the Young's Modulus and Poisson ratio of the indenter and of the small punch sample, respectively. Values of these characteristics are reported in Table 1.

b) The elastic bending deformation can be treated as the problem of a plate subjected to a deflection under a static loading. The solution of this type of problem has been solved analytically,

Table 1 Evolution of Poisson's ratio, Young's Modulus and yield stress with the temperature on WCo and 12Cr-1Mo steel.

		25°C	300°C	600°C
WCo	ν	0.3	0.3	0.3
(ball)	E (GPa)	240	235	200
	ν	0.33	0.33	0.33
12Cr-1Mo	E (GPa)	200	170	105
	σ_y (MPa)	435	375	250

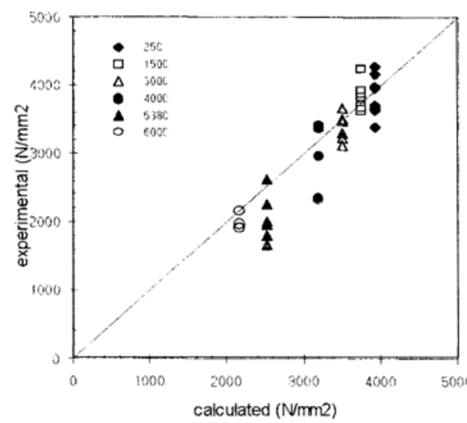

Fig. 2 Comparison between calculated and experimental SP elastic slope on austenitic 12Cr-1Mo steel.

and the equation relating the applied force, P, and the deflection, w, can be found in handbook (Pilkey, 1994) :

$$P = \frac{64Dw[1-(1-w^2)]^{1/2}}{1{,}540(d/2)^2(L/2)^4[C_1+2C_2(1+\alpha^2)+\alpha^4]} \qquad (3)$$

where C1, C2 and α are constants depending on the geometry, d is the ball diameter and D is the moment of inertia. This formulation takes into account of the geometry, of the evolution of the contact area between indenter and sample during deflection, and of the load distribution applied on the sample through the ball. This distributed load has been taken as:

$$p = P(1-x^2) \qquad (4)$$

and is expressed in Eq. (3) by the factor 1.504.

For the simulation of small punch experiments performed above room temperature, dilatations of the specimen, ball, and die were also taking into account. Results of the calculation are reported in Fig. 2 and compared with experimental values of the compliance. A satisfactory correlation between experiments and analytical theory of the small punch load-deflection slope has been found in the whole temperature range from 25° to 600° C.

2.2 Plastic bending regime

In the above analysis, the material behavior was assumed to be purely elastic. When the stress exceeds the yield stress, the mechanical behavior of metallic material diverges from linearity and the total deformation becomes the sum of an elastic and a plastic (inelastic) deformation. If the mechanical behavior of the material is known, we can calculate the load when the specimen is subjected to bending, using a plastic bending analysis. This implies that we should calculate the stress and strain within the sample. We will assume that stresses and strains are uniforme within the specimen cross-section. According to this assumption, and proceeding by small increment of the deflection, the stress is calculated by dividing the load, obtained from the elastic calculation, by the surface under the indenter. Having determined the stress, the stress-strain relationship as defined by uniaxial tensile test, can be applied. For stresses lower than the yield stress, the total strain is equal to the elastic strain and thus we obtain a relation between deflection and total strain. If the yield stress has been reached, the total strain is the sum of the elastic strain plus the plastic strain. Assuming that the jig, puncher, ball and testing machine are perfectly rigid, the deflection recorded is due exclusively to the deformation of the specimen, and considering the conservation of the volume, the deflection rate is proportional to the total strain rate. Therefore, we can determine the plastic strain and then calculate the real stress. The real load, as considered according to plastic bending, is calculated by multiplying the stress by the surface under the indenter. Using a spherical indenter, the radius of the contact area is obtained by the relation:

$$x^2+y^2=1 \tag{5}$$

where x $(=r)$ is the contact radius between the indenter and the specimen when the indenter is at a vertical position, y, equal to the deflection.

From the value of the load, Fe, determined from the above calculation using an elastic analysis, the stress under the indenter is equal to:

$$\sigma=\frac{1.504F}{4\pi r h_o/3} \tag{6}$$

where the constant 1.504 is expressing the distributed load on the sample, as in the elastic calculation, $4\pi r h_o/3$ is the specimen section on beneath the contact area, calculated from the initial thickness, h_o, and the radius of the contact area, r, related to the deflection by Eq. (5).

Knowing the total strain we can apply the stress-strain relationship to calculate the elastic and plastic strains within the sample. For the analytical description of the mechanical behavior, we used the constitutive equation proposed by Drucker-Prager (Drucker, 1988):

$$\dot{\varepsilon}_p=D\left(\frac{\sigma}{\sigma_y}-1\right)^p \tag{7}$$

where σy is the yield stress, and D and p are two constants dependent on the temperature. Both constants, D and p, were determined from uniaxial tensile test (UT) data published by Vigneron *et al.* (1988) and Ha (1994).

The evolution of Young's Modulus and yield stress in the temperature range 25° to 600°C is

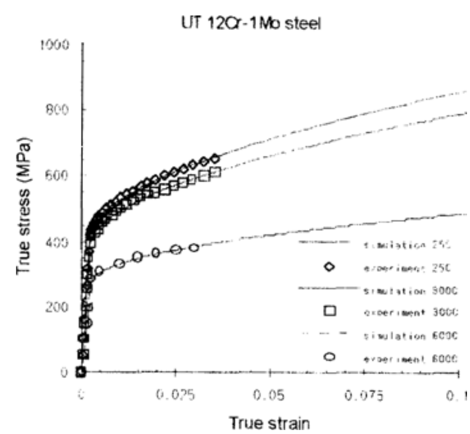

Fig. 3 Simulation of the UT mechanical behavior of 12Cr-1Mo steel.

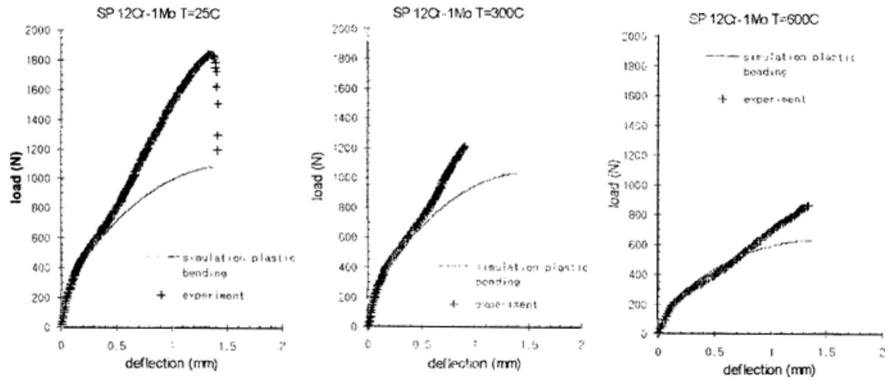

Fig. 4 Simulation of the SP plastic bending on austenitic 12Cr-1Mo steel at 25°, 300° and 600°C.

reported in Table 1 and the corresponding mechanical behavior is presented in Fig. 3.The small punch test load-deflection responses an calculated at 25°, 300° and 600°C, and results have been compared to experimental curves in Fig. 4.In the first two regimes, corresponding to elastic bending and plastic bending, the simulation gives a satisfactory agreement.

The calculated curves diverge from the small punch experimental behavior in the so-called membrane stretching regime because of a different nature of deformation. In the plastic bending, reflecting a biaxial strain state, the load increases as a consequence of the work hardening and of the increase in the contact area between ball-punch and specimen surface. On the other hand, the membrane stretching regime is resulting from the predominance of the radial strain, and therefore a different analysis should be made in order to describe this evolution of the strain state within the specimen during the small punch test.

2.3 Membrane stretching regime

The problem of a sheet stretched by a hemispherical punch while the sheet is clamped at the periphery is similar to the so-called 'cup test' commonly used in the sheet metal industry to assess the pressing quality of sheet metals.

A formulation has been proposed by Wang (1970) who analyzed the punch stretching test of sheet metal as a biaxial problem, and used a stress-strain incremental equation based on an Hill's plasticity theory.

Let's consider a circular sheet of radius ro and

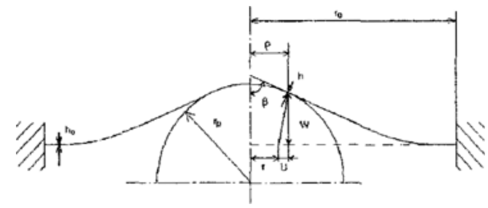

Fig. 5 Stretching of a sheet by a hemispherical punch.

of uniform thickness ho (Fig. 5). The sheet is clamped firmly along its periphery and then stretched by a hemispherical punch of radius rp, pushing at the center of the sheet. Suppose that at a certain stage in the stretching, a material element with initial radial distance, r, was displaced by a radial displacement, U, and an axial displacement, W. Then the radial and circumferential strains εr and $\varepsilon\theta$ become:

$$\varepsilon_r=\frac{1}{2}\ln\left[\left(1+\frac{dU}{dr}\right)^2+\left(\frac{dW}{dr}\right)^2\right] \qquad (8)$$

$$\varepsilon_\theta=\ln\left(\frac{\rho}{r}\right) \qquad (9)$$

where $\rho=r+U$ denotes the current radial distance. The strain within the thickness, εh, is given by:

$$\varepsilon_h=\ln\left(\frac{h}{h_0}\right)$$

where h and ho are, respectively, the current and initial thickness of the sheet.

The derivation of this problem is quite complex, so we will refer to the mathematical formulations obtained by Wang and Shammamy (1969). They obtained the two following expressions for the radial and circumferential strains.

$$\varepsilon_r = \frac{\varepsilon}{1+R}[(1+2R)^{1/2}\cos\phi - R\sin\phi] \quad (11)$$

$$\varepsilon_\theta = \varepsilon\sin\phi \quad (12)$$

where Φ is related to the principal stresses ϕ_r and ϕ_θ by the equation:

$$\phi = \arctan\left[\frac{1+R}{(1+2R)^{1/2}}\frac{\phi_\theta}{\phi_r} - \frac{R}{(1+2R)^{1/2}}\right] \quad (13)$$

where R denotes the strain ratio as defined by Hill, i. e. $R = d\varepsilon_2/d\varepsilon_3$.

Knowing the punch displacement, we can determine $\rho = r + U$ and therefore the circumferential strain, ε_θ, then total strain, ε, and finally the radial strain, ε_r, from the Eq. (11) and Eq. (12). By applying the stress-strain relationship, $\sigma = f(\varepsilon)$, we can therefore calculate the punch load if we know the contact radius between the ball and the specimen. The punch load P can be calculated by integratihy over the entire contact region in the direction parallel to the axis of symmetry:

$$P = \frac{2}{\sqrt{3}}\pi\mu\rho(r_s)\,h(r_s)\,\frac{\sigma_r(r_s)}{r_o} \quad (14)$$

where $\rho(r_s)$, $h(r_s)$ and $\sigma(r_s)$ are calculated at the ball-sample contact boundary radius, r_s, and μ is the coefficient of friction ball/specimen. The expression used for the calculation of the evolution of the thickness during test was:

$$\varepsilon_h = -\frac{1}{4}(\varepsilon_r + \varepsilon_\theta) = \ln\left(\frac{h}{h_o}\right) \quad (15)$$

Calculations were performed by small incremental increase of the deflection. The evolution of the radial and circumferential strains, as calculated at T=25°C, has been reported in Fig. 6.The stress and strain state within the small punch sample is thus quite complex, with a larger increase of the median strain in comparison to the circumferential strain. Measurements in the median and circumferential strains were performed during punch stretching by Hecker (1977) using grids photoprinted on the surface of metallic sheets. Strains calculated with the Wang's formulation are found to follow similar evolution than the strains measured experimentally, with a larger circumferential strain for small punch test.

This calculation is also taking into account of

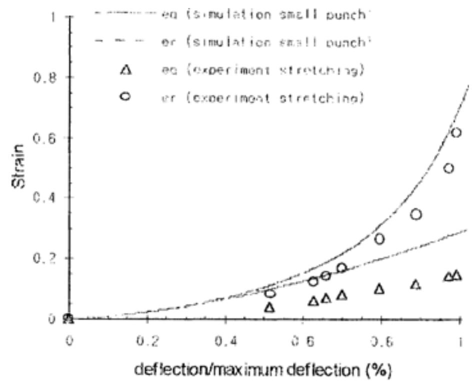

Fig. 6 Evolution of the calculated strains εr and $\varepsilon\theta$ in small punch test and comparison with experimental measurements performed in punch stretching (Hecker, 1977).

Table 2 Values of the coefficient of friction.

Temperature	25°C	300°C	600°C
coef. of friction	0.99	0.96	0.84

the friction between the ball and the specimen. Values used for this calculation are reported in Table 2. It has been assumed that only slight friction exists between the ball and the surface of specimen at T=25°C, and that this friction is increasing with the temperature. The formation of an oxide layer at the specimen surface, during the exposition at high temperature, is justifying this assumption.

The small punch test load-displacement simulation is based on the knowledge of the stress-strain mechanical behavior, generally determined from uniaxial tensile test. For this purpose, the Drucker-Prager constitutive formulation has been used, as presented in the paragraph related to the plasticity bending regime.

Results of the simulation are presented in Fig. 7 in the range of temperature 25° to 600°C. Assuming that the uniaxial stress-strain behavior is known, the Wang's formulation gives an accurate description of the membrane stretching regime in the whole range of temperature studied.

However, the divergence observed between simulation and experimental curve is interpreted as the influence on the mechanical behavior of the necking formation, and of the crack initiation and

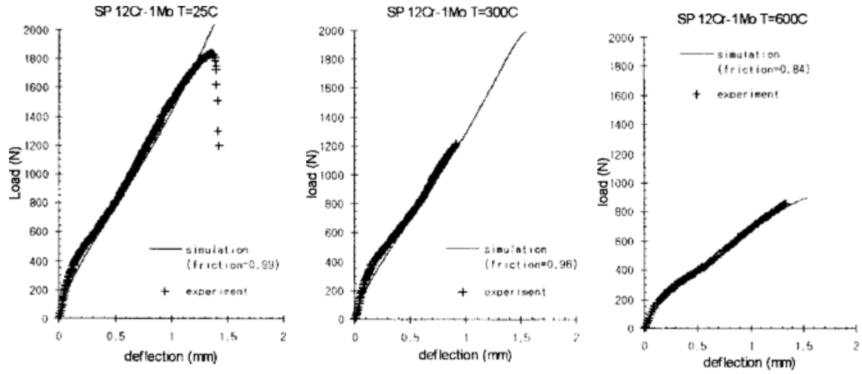

Fig. 7 Simulation of the SP membrane stretching regime on 12Cr-1Mo at 25°, 300° and 600°C.

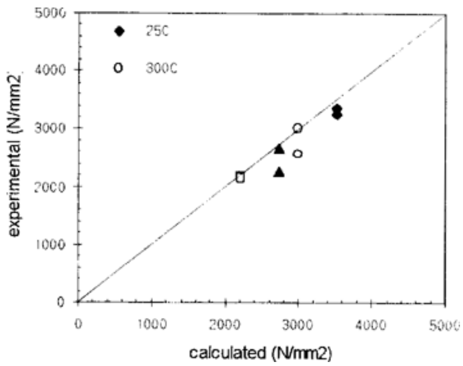

Fig. 8 Comparison between calculated and experimental SP elastic slope on ferritic 1Cr-0.5Mo ex-service steel.

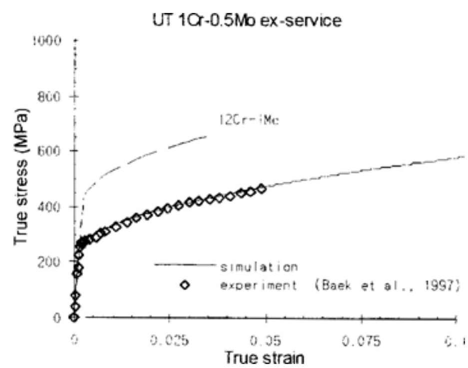

Fig. 9 Simulation of the UT mechanical behavior of ex-service 1Cr-0.5Mo steel at T=25°C, and comparison with the austenitic 12Cr-1Mo steel.

propagation leading to the failure of the small punch specimen.

3. Application of the Equations to Ferritic Steels

The validity of the equations has been examined by small punch tests performed on ex-service 1Cr-0.5Mo steel, as described in Part-I (Ha et al., 1998). Figure. 8 shows that the elastic calculation of the compliance gives a good prediction of the small punch elastic compliance within the whole temperature range.

For the simulation of the two following regimes, constants of the Drucker-Prager stress strain constitutive equation have been determined from uniaxial tensile test data, performed by Baek et al. (1997) at 25°C with a strain rate of $10^{-4}s^{-1}$ (Fig. 9).

The simulated load-deflection curves in the plastic bending and membrane stretching regimes are compared with the experimental data in Fig. 10, showing a good agreement.

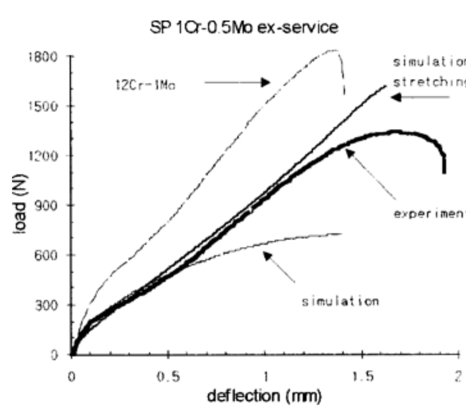

Fig. 10 Simulation of the SP behavior in the plastic bending and membrane stretching regimes of ex-service 1Cr-0.5Mo steel at 25°C, and comparison with 12Cr-1Mo.

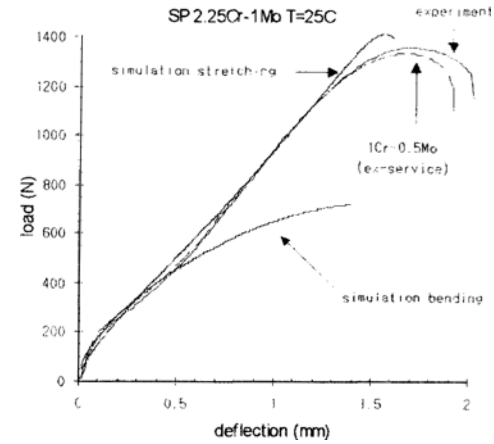

Fig. 11 Experimental SP load-deflection response on 2.25Cr-1Mo with fitting of the calculated plastic bending and membrane stretching curves, and comparison with 1Cr-0.5Mo steel.

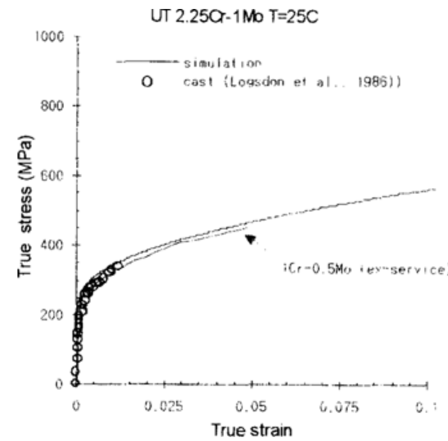

Fig. 12 Simulation of the UT mechanical behavior of 2.25Cr-1Mo wrought steel, and comparison with cast 2.25Cr-1Mo and 1Cr-0.5Mo steel.

From the results of the small punch load-deflection curves obtained from materials having different mechanical behavior, it appears that a decrease of the yield stress leads to a decrease of the load in the plastic bending, a decrease of the strain hardening to a decrease of the slope in the membrane stretching curve, and a decrease of the ultimate tensile strength to a decrease of the maximum load. The proposed formulations described accurately the influence of these mechanical characteristics.

Results of these simulations, performed on two low alloy steels having a relatively large difference of mechanical behavior. This suggests that the analytical formulations might be used successfully to a wider array of material.

The load-deflection response obtained from small punch test can also be used to assess the material stress-strain behavior. In this case, constants of the constitutive equation, used to describe the stress-strain response, can be determined by matching the experimental small punch test response with the simulated plastic bending and membrane stretching curves.

This procedure has thus been applied to the ferritic 2.25Cr-1Mo steel (Fig. 11). Both constants, D and p, of the Drucker-Prager constitutive equation were determined by superposing the experimental small punch test curve with the simulated curves obtained from the equations proposed to describe the plastic bending and membrane stretching regimes. The predicted stress-strain mechanical behavior has been reported in Fig. 12, and compared with tensile test data obtained on 2.25Cr-1Mo cast steel by Logsdon *et al.* (1986). The constitutive parameters predicted from small punch test load-displacement lead to a stress-strain curve slightly above to the uniaxial tensile stress-strain curve determined experimentally on cast material.

Results obtained for both ferritic steels showed that their mechanical behaviors are very similar, with 2.25Cr-1Mo steel having a slightly higher value of the yield stress in comparison with 1Cr-0.5Mo steel, but identical strain hardening coefficients.

Therefore, this procedure produces stress-strain curve and properties predictions closely resembling standard tensile test curves.

4. Conclusions

The development of the small punch technique to assess the mechanical behavior has been described.

Compliance curves obtained on disks demonstrated good agreement between analytical theory and experimental observations. Using the Drucker-Prager constitutive model and taken into account of the friction between indenter and small punch sample, the plastic bending and membrane regime could also be predicted satisfactoring in the temperature range from 25° to 600°C.

It was therefore suggested that small punch test load-deflection could be used to evaluate the mechanical behavior when the tensile stress-strain curve and mechanical properties are unknown. This offers to the small punch test considerable potentialities, as also to evaluate the remaining mechanical behavior of aged material.

Acknowledgement

The Commission of the European Union is acknowledged for the financial support of Dr. E. Fleury at the Korea Electric Power Research Institute.

References

Baek S. G., Song G. S and Hyun J. S., 1997, "A Study on the Interactive Effect of Crep-Fatigue in Boiler," KEPRI Technical Report No. TR. 95YS01.97.36 (in Korean)

Baik J. M., Kameda J., and Buck O., 1986, "Development of Small Punch test for Ductile -Brittle Transition Temperature Measurement of Temper Embrittled Ni-Cr Steels," *The Use of Small-Scale Specimens for Testing Irradiated Material, ASTM STP 888*, W. R. Corwin and G. E. Lucas, Eds., American Society for Testing Materials, Philadelphia, U. S. A., pp. 92～111.

Drucker D. C., 1988, "Conventional and Unconventional Plastic Response and Representation," *Applied Mechanical Review*, 41, pp. 151～167.

Foulds J. R. and Viswanathan R., 1994, "Small Punch testing for Determining the Material Toughness of Low Alloy Steel Components in Service," *Journal of Engineering Materials and Technology*, Vol. 116, pp. 457～464.

Ha J. S., 1994, "Thermal-Mechanical Fatigue Behavior and Life Prediction of 12 Cr steel," Ph. D. Thesis, Chungman National University, Taejon, South-Korea (in Korean).

Ha J. S. and Fleury E., 1998, "Small Punch Test on Steels for Steam Power Plant(I) Ductile -Brittle Transition temperature," *KSME International Journal*.

Hecker S. S, 1977, "Experimental Studies of Sheet Stretchability," in proceedings of the Conference *Formability: Analysis, Modeling, and Experimentation*, S. S. Hecker, A. K. Ghosh, and H. L. Gegel, Eds., held in October 24-25th, 1977, Chicago, IL, USA, pp. 150～182.

Huang F. H., Hamilton M. L., and Wire G. L., 1982, "Bend Testing for Miniature Disks," *Nuclear Technology*, Vol. 57, May 1982, pp. 234～242.

Logsdon W. A., Liaw P. K., Saxena A. and Hulina V. E., 1986, "Residual Life Prediction and Retirement for Cause Criteria for SSTG Upper Casings, Part-I: Mechanical and Fracture Mechanics Material Properties Development," *Engineering Fracture Mechanics*, Vol. 25, No. 3, pp. 259～288.

Lucas G. E., 1990, "Review of Small Specimen Test Techniques for Irradiation Testing," *Metallurgical Transactions A*, Vol. 21A, May 1990, pp. 1105～1119.

Manahan M. P., Argon A. S., and Harling O. K., 1981, "The development of a Miniaturized Disk Bend Test for the Determination of Post -irradiation Mechanical Properties," *Journal of Nuclear Materials*, Vol. 103-104, pp. 1545～1550.

Mao X, Shoji T. and Takahashi H., 1987, "Characterization of Fracture Behavior in Small Punch Test by Combined Recrystallization-Etch Method and Rigid Plastic Analysis," *Journal of Testing Evaluation*, Vol. 15, pp. 30～37

Onat E. T. and Haythornthwaite R. M., "The Load-Carrying Capacity of Circular Plates at Large Deflection," *Journal of Applied Mechanics*, Vol. 23, March 1956, pp. 49～55.

Pilkey W. D., 1994, "Formula for Stress, Strain, and Structural Matrices," Ed., Wiley Interscience Publication.

Vigneron G., Vandershaeghe A. and Lecoq J., 1988, "A Metallurgical Contribution to the Industrial Development of 12% Chromium Martensitic Steels for Pressure Vessels," *Int. J. Pressure*

Vessels & Piping, 32, pp. 389~413.

Wang N. M., 1970, "Large Plastic Deformation of a Circular Sheet Caused by Punch Stretching," *Journal of Applied Mechanics, Transaction of the ASME*, paper No. 70-APM-KK, June 1970, pp. 431~440.

Wang N. M. and Shammamy M. R., 1969, "On the Plastic Bulging of a Circular Diaphragm by Hydrostatic Pressure," *J. Mech. Phys. Solids*, Vol. 17, pp. 43~61.